



# LUND UNIVERSITY

## Wood Composition Based on Recycled Plastic - Mechanical Properties

### Report from Luleå Institute of Technology

Nilsson, L.O.; Hjort, S.; Petterson, H.; Gustavsson, P.J.; Molin, N. E.; Sjö Dahl, M.; Ståhle, P.; Gunnars, J.; Ericson, M.; Vilander, K.; Lindberg, H.

1997

#### Document Version:

Publisher's PDF, also known as Version of record

[Link to publication](#)

#### Citation for published version (APA):

Nilsson, L. O., Hjort, S., Petterson, H., Gustavsson, P. J., Molin, N. E., Sjö Dahl, M., Ståhle, P., Gunnars, J., Ericson, M., Vilander, K., & Lindberg, H. (1997). *Wood Composition Based on Recycled Plastic - Mechanical Properties: Report from Luleå Institute of Technology*. Luleå University of Technology.

#### Total number of authors:

11

#### Creative Commons License:

Unspecified

#### General rights

Unless other specific re-use rights are stated the following general rights apply:

Copyright and moral rights for the publications made accessible in the public portal are retained by the authors and/or other copyright owners and it is a condition of accessing publications that users recognise and abide by the legal requirements associated with these rights.

- Users may download and print one copy of any publication from the public portal for the purpose of private study or research.
- You may not further distribute the material or use it for any profit-making activity or commercial gain
- You may freely distribute the URL identifying the publication in the public portal

Read more about Creative commons licenses: <https://creativecommons.org/licenses/>

#### Take down policy

If you believe that this document breaches copyright please contact us providing details, and we will remove access to the work immediately and investigate your claim.

LUND UNIVERSITY

PO Box 117  
221 00 Lund  
+46 46-222 00 00

# Wood Composites Based on Recycled Plastics - Mechanical Properties

<sup>1</sup>L.-O. Nilsson, <sup>1</sup>S. Hjort, <sup>2</sup>H. Petterson, <sup>2</sup>P.-J. Gustavsson, <sup>3</sup>N.-E. Molin, <sup>3</sup>M. Sjö Dahl, <sup>4</sup>P. Ståhle, <sup>4</sup>J. Gunnars, <sup>5</sup>M. Ericson, <sup>6</sup>K. Oksman, <sup>6</sup>Y. Vilander and <sup>6</sup>H. Lindberg

## 1. Introduction and Background

Polypropylene, PP, is a synthetic polymer widely used in injection molded products. In recent years the use have changed from simple products to engineering products replacing acetals and nylons in for example cars. The successful replacement follow from a manipulation of the structure in order to overcome its demerit of bad mechanical properties below freezing point. In our case it is worth to remember that the mechanical properties as Young's modulus is very low for the pure material. The material is hydrophobic depending of that the molecules give only dispersion forces (London, van der Waals). The material is frequently used as a water, water vapour, barrier material. The material is abundant and cheap and occur frequently in recycled material trade. It is also noteworthy that the material can be polymerised, without additives, from wood. This is not an economic alternative to the used oil or gas polymerisation. Sawdust is an abundant and cheap reinforcing material or filler. In addition sawdust have a large surface area of about 200 m<sup>2</sup>/Kg. Sawdust can be used for increasing Young's modulus of PP and research have been conducted for this type of material combination in order to replace PP with common fillers with recycled PP and sawdust. However, wood molecules exhibit a hydrophilic character, wood polymers add to dispersion forces polar forces from hydroxyl groups. This results in incompatibility between sawdust and PP. The resulting poor mechanical properties as strength, elongation to break, impact properties can be overcome by adding a small amount of compatibiliser, for example a block copolymer where one block is compatible with the PP matix and the other block is compatible with the wood.

In present work the aim is to increase the knowledge about research paradigms of the different research areas involved and presentation of the instrumentation found in the different departments. In order to reach the goal two types of methods were used. Firstly several work meetings were performed at the different research locations. The workshops discussed the research at the location and study the research equipment. Secondly a round robin test of a dummy material was performed. The material was injection molded PP with sawdust of different concentrations. The material was not compatibilised for optimal mechanical properties.

The present project has the form of a Round Robin, whereas a subset of the investigated properties have been determined by more than one of the groups. This enables a comparison of methods and results.

<sup>1</sup>Building Materials, Chalmers Institute of Technology, <sup>2</sup>Structural Mechanics, Lund Institute of Technology, <sup>3</sup>Experimental Mechanics, <sup>4</sup>Solid Mechanics, <sup>5</sup>Polymer Technology, <sup>6</sup>Wood Technology, Luleå University of Technology

## 2. Material Description

### 2.1 Characterisation of the material

Polypropylene (PP)/wood flour (WF) composites were fabricated with fibre weight fractions of 0, 0.20 and 0.40. Two different PP homopolymers with different melt flow index (MFI) were used. To improve processing additives were used according to the recommendations from the material supplier. The materials are described in Table 2.1 and the formulations are given in Table 2.2.

Table 2.1. Material used in the study

| Material         | Description   | Supplier  |
|------------------|---|---|
| PP1              | PP homopolymer<br>MFI = 4 g/10 min<br>Trade name: "Fortilene 9200"    | Solvay Polymers Inc.<br>Deer Part, Texas, USA       |
| PP2              | PP homopolymer<br>MFI = 36.5 g/10 min<br>Trade name: "Fortilene 3907" | Solvay Polymers Inc.<br>Deer Part, Texas, USA       |
| Wood flour (WF)  | 40 mesh pine (#4020)  | American Wood Fibres<br>Schofield, WI, USA          |
| Calcium stearate |   | Syncro-Synthetic Products<br>Co. Cleveland, OH, USA |
| Antioxidant      | "Irganox 1010"  | Ciba-Geigy<br>Hawthorne, NY, USA                    |

Table 2.2. Formulations of composites

| Material    | Blends 0 | Blend 0,20 | Blend 0.40 |
|-------------|----------|------------|------------|
| PP (kg)     | 9.94     | 7.95       | 5.96       |
| WF (kg)     | 0        | 2.00       | 4.00       |
| Ca Stearate | 0.050    | 0.040      | 0.030      |
| Antioxidant | 0.010    | 0.008      | 0.006      |

## 2.2 Processing of composites

The wood flour was dried in a steam heated dryer for a minimum of 4 hours. The wood flour, PP and additives were then compounded in a 32 mm, 20 L/D, Davis Standard Corporation (Pawcutuck, CT) co-rotating, intermeshing twin screw extruder (Screw design #2). The extrudate was water cooled with a water spray and cut to pellets.

Compounded pellets were dried for a minimum of 4 hours at 105 °C and then injection moulded using a 33 ton, reciprocating screw, injection moulder (Cincinnati Milacron, Batavia, OH). 6.5 mm thick plaques were moulded for further testing. The temperatures in the injection moulding machine were 290 °C in feed zone, zone 2 and zone 3. The temperature of the nozzle was 275 °C. The injection time was 15 seconds, the packing time 5 seconds, the holding time 20 seconds and the total cooling time 35 seconds.

## 2.3 Visual characterisation of the material

Fibre angles are measured for PP1 and PP2 with 20% fibre content. The experimental procedure is as follows: Sections representing area I-IV, are sawn from the specimen and cut into samples with size 25 × 2,5 mm<sup>2</sup>. The samples are gradually sectioned from the surface to the centre. L0 indicates the surface and L8 the centre layer. Layer thickness is 0,4 mm. Fibre angles are measured for each layer, assuming equal fibre orientation on each side of the centre line. The reference angle 0° is equal to the injection direction, i.e. vertical in Fig. 2. Area A and B represents positive and negative angles respectively.

Results are presented in Table 2.3.

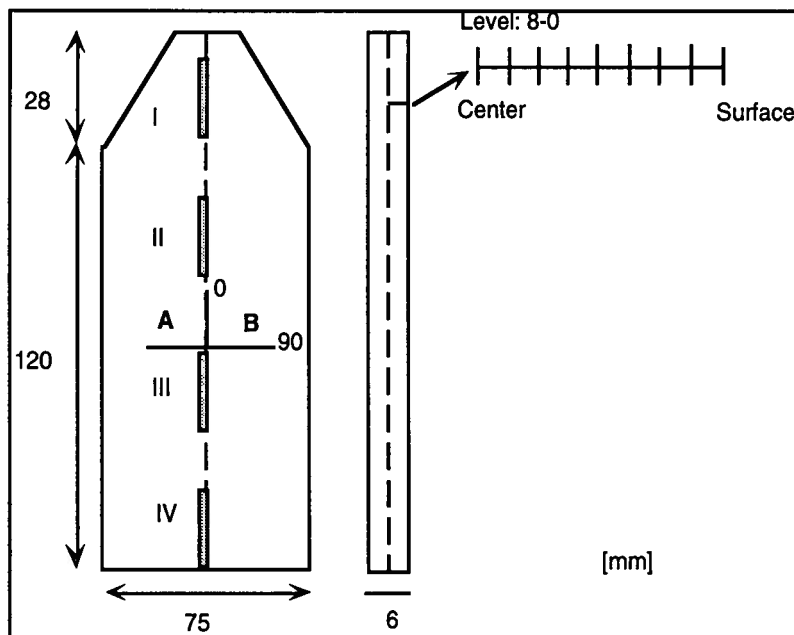


Fig. 2 The dimensions of the material as manufactured.

Table 2.3

| Area | Level | Description  |
|------|-------|--|
| I    | 0-6   | Approximately isotropic distribution                     |
|      | 7-8   | Main part of the fibres in 30-60° positive direction (A) |
| II   | 0-3   | Approximately isotropic distribution                     |
|      | 4-6   | Fibres in area A60° to B50°                              |
|      | 7-8   | Distribution from A60° to B70°                           |
| III  | 0-3   | Approximately isotropic distribution                     |
|      | 4-6   | Distribution from A70° to B40°                           |
|      | 7-8   | Distribution from B40° to B80°                           |
| IV   | 0-1   | Approximately isotropic distribution                     |
|      | 2-4   | Distribution from A60° to B60°                           |
|      | 5-6   | Distribution from A70° to B60°                           |
|      | 7-8   | Distribution from A80° to B70°                           |

### 3. Young's Modulus and Poisson's Ratio and Anisotropy

The measurements reported in this section were performed using optical measuring methods. Using Electronic Speckle Photography a quasi-static response of the material for a one-axial tensile test was investigated, and using TV-holography the anisotropy of the materials both from modal analysis and transient bending wave propagation were examined. The geometry of the test material was, however, not optimal for the latter experiment therefore no useful information was obtained. A better object would have been a thinner and wider plate.

The response during the quasi-static tensile test was measured using Electronic Speckle Photography. A modification of the non-contacting optical technique has been developed at the department. Six samples of the dimension 149×33×6 mm<sup>3</sup> were cut out and pulled along the main axis of the wood fibres (the stiffest direction) in an Instron tensile test machine at the constant speed of 0.01 mm/s. No additional object preparation was necessary. The texture in the composites gave a random structure which was enough for the method to work. The result from the measurements are seen in Table 3.1. The variation of Poisson's ratio with increasing stress was found negligible. The values of Poisson's ratio in Table 3.1 are

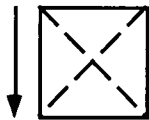
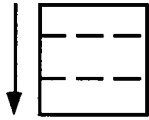

Table 3.1.

| Material | Young's Modulus [MPa] | Poisson's ratio |
|----------|-----------------------|-----------------|
| PP1 00%  | 1380                  | 0.41(3)         |
| PP1 20%  | 2250                  | 0.37(3)         |
| PP1 40%  | 3200                  | 0.30(4)         |
| PP2 00%  | 1360                  | 0.41(9)         |
| PP2 20%  | 2300                  | 0.35(6)         |
| PP2 40%  | 3100                  | 0.26(6)         |

therefore the mean values over the load cycle. Young's modulus on the other hand decreased monotonically with increasing stress in all six material combinations, which implies a viscoelastic effect. The values in Table 3.1 are the initial Young's modulus, which dropped to about 90 % for the matrix material alone and 80 % for the composite materials before fracture, respectively. In the two composites with 40 % wood fibre, an initial increase in stiffness with stress of about 10 % was found before the decrease because of the viscoelasticity started to dominate. The maximum stiffness in both these materials were obtained at 7.5 MPa.

The anisotropy of the wood composite materials was examined using modal analysis with TV-Holography. The six plates were cut into squares with the side equal to the original plate width, and put, simply supported, in front of a loudspeaker connected to a tone generator. The two matrix materials alone were found to be almost isotropic, while the composites seem to be orthotropic with a relation between the stiffest direction (along the principal manufacture direction) and the weakest of approximately 1.6 regardless of matrix material and wood fibre concentration. The used mode shapes and obtained frequencies are shown in Table 3.2.

Table 3.2.

| Modal shape   | PP1 0% [Hz] | PP1 20% [Hz] | PP1 40% [Hz] | PP2 0% [Hz] | PP2 20% [Hz] | PP2 40% [Hz] |
|---|-------------|--------------|--------------|-------------|--------------|--------------|
|  | 2240        | -            | -            | 2200        | -            | -            |
|  | -           | 2240         | 2670         | -           | 2490         | 2670         |
|  | -           | 1880         | 2080         | -           | 1990         | 2130         |

The arrows in Table 3.2 indicates the stiffest direction. The results listed in Table 3.1 and Table 3.2 are consistent whereas both indicate an increase in stiffness of nearly 40% by increasing the wood content from 20% to 40%.

The measuring methods used here are, compared to conventional techniques, both fully non-contacting (no object preparation is necessary) and field measuring, giving the deformation in all points on the object surface simultaneously without being in contact with the object. In addition, both Young's modulus and Poisson's ratio are measured simultaneously and all three modal shapes were obtained in the same set-up.

#### 4. Creep Properties

For creep test and tensile test two 12 mm wide rectangular-shaped specimens were machined with an Accutom (from Struers) from the central part of the moulded plates. A 4.2 MPa constant stress was applied at constant temperature (ambient) for 105 seconds. The strain was continuously recorded by means of an Instron extensometer connected to a PC. The creep modulus as function of time was calculated as the stress/strain ratio using the nominal cross-section area.

The tensile tests were performed in an Instron testing apparatus. Two different cross-head speeds of 2 mm/min and 20 mm/min were used. The Young's modulus was determined from the linear part of the stress-strain curve and the peak stress was the peak load divided with the unloaded cross-section area.

The creep modulus as function of time is plotted in Fig. 4.1 for PP1 and Fig. 4.2 for PP2. The fibre content change the creep rate and the creep modulus significantly. The higher the fibre content the higher modulus and creep rate. As seen in Figs. 4.1 and 4.2 the creep modulus for each fibre content is not significantly different for the two matrix materials. So, the difference in molecular weight between PP1 and PP2 is not sufficient to give a difference in creep modulus.

In Fig. 4.3 Young's modulus and in Fig. 4.4 the fracture stress from the tensile test are presented. Both the strain rate and fibre content show effect on both Young's modulus and the fracture stress. The higher strain rate and fibre content result in the higher Young's modulus and a lower fracture stress. However the different matrix materials show no significant effects.

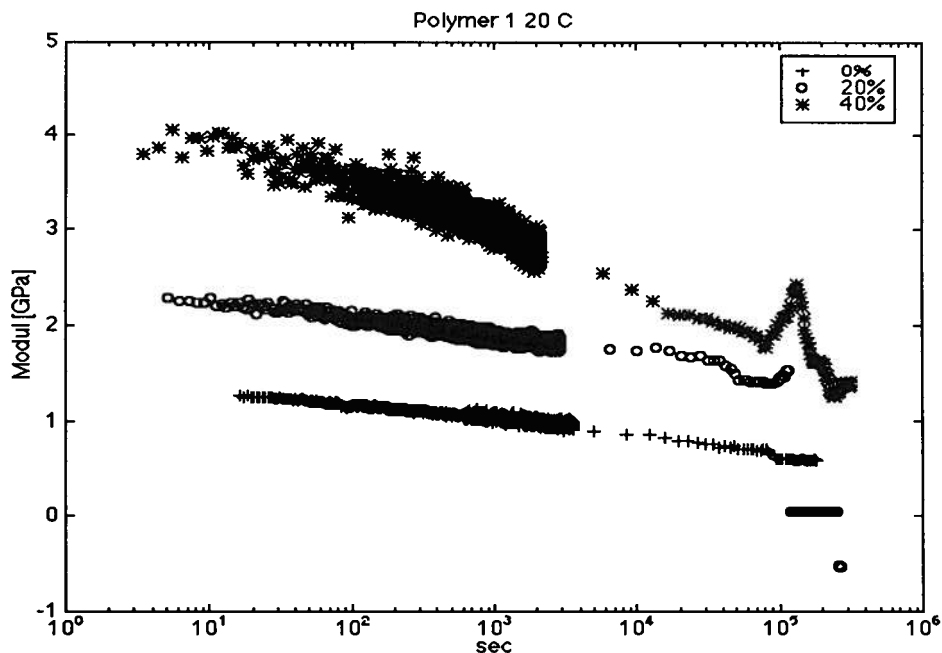


Fig. 4.1. creep modulus versus time for PP1.

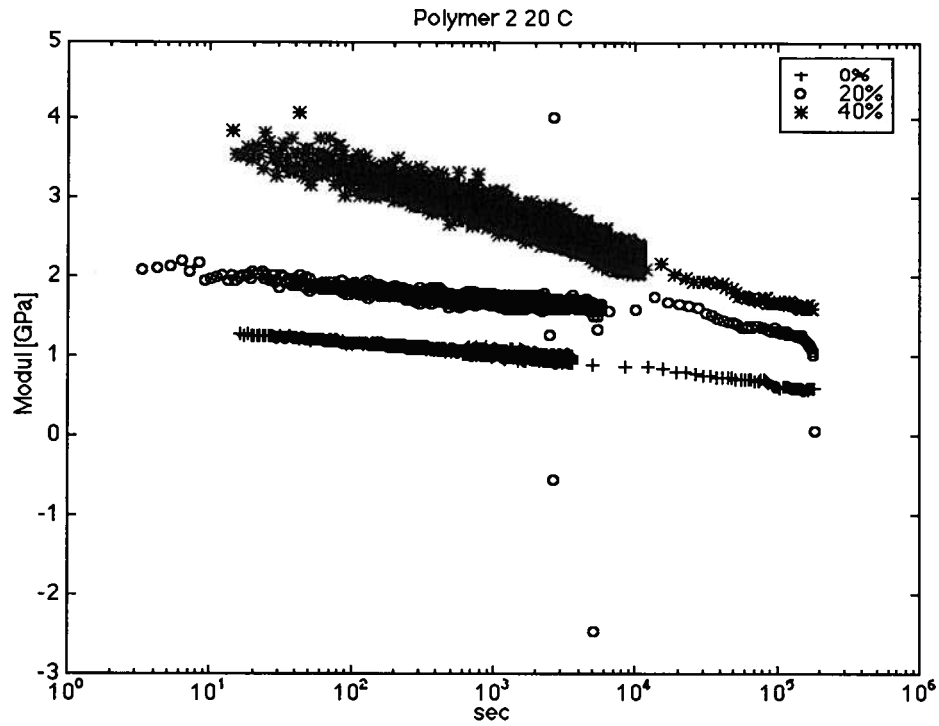


Fig. 4.2. creep modulus versus time for PP2.

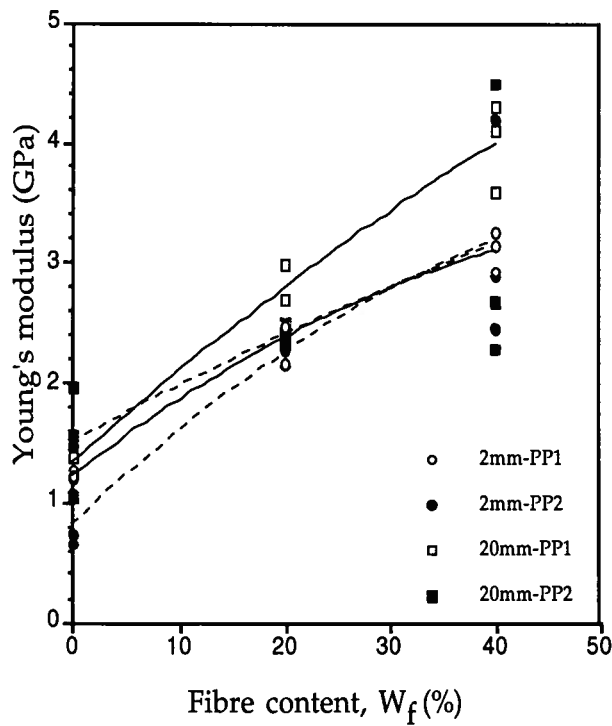


Fig. 4.3. Young's modulus versus fibre content.

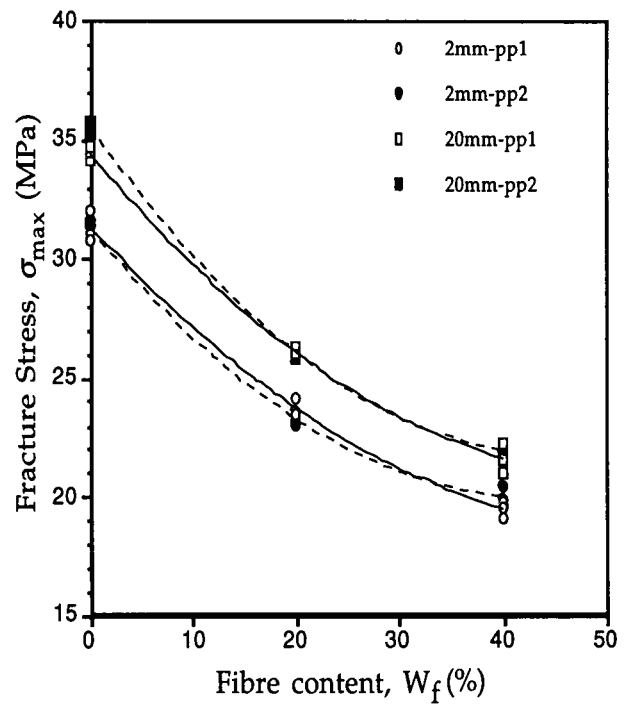


Fig. 4.4. Fracture stress versus fibre content.



## 5. Static Young's Modulus, Tensile Strength, Notch Sensitivity and Fracture Energy

### 5.1 Young's modulus and tensile strength

The test of stiffness and strength was carried out as a tensile test of bone-shaped specimens. The ends of the specimens were clamped between two steel plates. The plates were attached to the actuators of the testing machine by chains. In this way a centric tensile loading was achieved. The cross-head rate of the machine was 1.0 mm/min giving a strain rate in the material in the order of 1%/min. The temperature and relative humidity in the testing room was about 22°C and 40%, respectively. The size of the cross-section was nominally 6 mm times 20 mm, and the length of the part of the specimen with this constant cross-section about 60 mm. The strain was obtained by measuring the elongation along 40 mm by two LVDT:s placed symmetrically at opposite sides of the cross-section. The tensile strength of the material,  $f_t$ , was evaluated as recorded maximum load divided by the initial size of the cross section at zero load. Young's modulus was obtained from the slope of the stress-strain curve, the stress calculated as recorded force divided by initial cross-section size and the strain as the recorded elongation divided by the gauge length, 40 mm. The slope of the curve was obtained from the change in stress and strain from about 5% and to about 30% of the tensile strength. In this region the performance of materials tested was very close to linear and the slope probably very close to the tangential stiffness in origin. In Table 5.1 the test results for strength and stiffness are indicated in the form of the mean result from three nominally equal tests of each material. The scatter in the results within each series of three tests was small, the mean of the coefficients of variation being 2.6%.

Table 5.1 Young's modulus and tensile strength of the six materials tested.

|                              | PP1-<br>0% | PP1-<br>20% | PP1-<br>40% | PP2-<br>0% | PP2-<br>20% | PP2-<br>40% |
|------------------------------|------------|-------------|-------------|------------|-------------|-------------|
| Young's Modulus, MPa         | 1390       | 2490        | 3950        | 1540       | 2090        | 3160        |
| Tensile Strength $f_t$ , MPa | 30.3       | 23.1        | 21.3        | 30.6       | 22.6        | 19.6        |

### 5.2 Notch sensitivity

The notch sensitivity tests were carried out by the same equipment and at the same conditions as the tensile test of specimens in homogeneous tension. The nominal free volume between clamped edges was for the notch sensitivity specimens length x width x thickness = 60 x 75 x 6 mm<sup>3</sup>. The centric tensile load was applied in the length direction. Three kinds of notches were tested:

- A symmetrical pair of sharp edge-notches placed symmetrically in the specimen, the depth of each notch being 9 mm, giving a nominal cross-section size equal to  $57 \times 6 \text{ mm}^2$ . The first 6 mm of each notch was made by a saw and had a width of about 1 mm. The last 3 mm of each notch was cut by a razor-blade.
- As the first kind of notch, but each notch being 18 mm deep, giving a nominal cross-section size equal to  $39 \times 6 \text{ mm}^2$ .
- As the second kind of notch, but the width of each notch being 10 mm and with a circular end shape of the notch, the diameter of the circle being 10 mm. The notch was manufactured by means of a saw and a drilling machine. The nominal cross-section size is  $39 \times 6 \text{ mm}^2$ .

For each combination of notched specimen geometry and material two nominally equal tests were made. With exception for the specimens with 0% wood and with a sharp notch, the scatter in the test results within each group was small, typically with a coefficient of variation about 2%. The specimens with 0% wood and a sharp notch showed a much greater scatter with coefficient of variations in the order of 10%. In Table 5.2 the results are shown as the ratio between the strength of the notched specimen to the strength of the un-notched specimen. The absolute values of the strength of the un-notched specimens are for the different materials given in Table 5.1.

In all cases the strength is evaluated as the maximum recorded load divided by the size of the net cross-section.

Table 5.2 Relative strength of specimens with a notch.

|                 | PP1-<br>0% | PP1-<br>20% | PP1-<br>40% | PP2-<br>0% | PP2-<br>20% | PP2-<br>40% |
|-----------------|------------|-------------|-------------|------------|-------------|-------------|
| un-notched      | 1.00       | 1.00        | 1.00        | 1.00       | 1.00        | 1.00        |
| a=9mm, r<0.1mm  | 0.75       | 0.99        | 0.86        | 0.59       | 0.86        | 0.85        |
| a=18mm, r<0.1mm | 0.81       | 1.00        | 0.88        | 0.61       | 0.88        | 0.89        |
| a=18mm, r=5mm   | 1.07       | 1.01        | 0.88        | 1.02       | 0.90        | 0.96        |

### 5.3 Fracture energy

A few left over specimens were used for single notch three point bending tests to determine the fracture energy of some of the materials. The fracture energy was determined as the total work of fracture, obtained as the area under the recorded load deflection curve from zero load at the start of the test to zero load after complete fracture of the specimen, divided by the size of the net cross-section area. To get sufficient length of the specimens, the steel plates used in the tensile tests were clamped on to the plates to be tested. In this way, a bend testing specimen with 250 mm distance between the supports (one roller support and one ball support), a height of 75 mm and a thickness of about 6 mm was achieved. The depth of the notch placed at the centre of the beam was 45 mm, making the net cross-section size equal to about  $30 \times 6 \text{ mm}^2$ .

The cross-head speed was 2 mm/min. This rate of loading gave a time to maximum load of about 1-2 minutes and a time to complete fracture of about 10 minutes. In all cases the course of failure was stable, meaning that there was no sudden decrease in load during the gradual increase in deflection. Final collapse at zero external load occurred due to the dead-weight of the specimen. Only four specimens were tested: no specimen with 0% wood content, no PP1-20%, two PP1-40%, one PP2-20% and one PP2-40%.

In Table 5.3 the fracture energy values obtained are indicated together with the nominal bending stress at maximum load. For a specimen with a geometry exactly equal to the nominal geometry, the nominal bending stress at maximum load is calculated as  $(\text{max load} \times 250 \text{ mm} / 4) \times (6 \times 30^2 \text{ mm}^3 / 6)$ . From this stress value the fracture toughness and the critical energy release rate of the material can be calculated, assuming linear elastic fracture mechanics for isotropic materials to be valid and using the stiffness values given in Table 5.1. The two tests of PP1-40% suggests that the scatter in tests results is small: the deviation between the two test recordings was less than 1% both for the fracture energy and for the maximum load.

Table 5.3 Fracture energy and nominal bending strength.

|                          | PP1-0% | PP1-20% | PP1-40% | PP2-0% | PP2-20% | PP2-40% |
|--------------------------|--------|---------|---------|--------|---------|---------|
| $G_f$ , J/m <sup>2</sup> | –      | –       | 10450   | –      | 12700   | 8000    |
| $f_{net}$ , MPa          | –      | –       | 34.1    | –      | 32.0    | 30.2    |

#### 5.4 Remark on general fracture performance

The materials without any wood fibres were seen to perform in a very ductile manner when tested without any notch. After peak load, necking of the specimen started. This necking did not lead to local failure, but instead the necking region extended along the entire length of specimen. Final failure was sudden and occurred at strain of about 400% and at a true stress in the order of 100 MPa. For specimens with a notch the performance was very different: the failure was brittle and sudden, and not preceded by yielding. In this case also the scatter in recorded tensile strength became much greater.

The specimens with wood fibres performed very different. They did not expose the same extreme ductility when tested without any notch, neither did they expose the very brittle and sudden failure when tested with a notch. From the test recordings and the general fracture performance it seems that the size of the fracture process region at the tip of a crack is much greater for the materials with particles, i.e., wood fibres, than for the pure plastic materials. The strain capacity before local peak stress seems on the other hand to be much greater for the materials without particles.

## 6. Young's Modulus, Tensile Strength and Fracture Strain at Different Temperatures and Different Strain Rates

Standard tensile tests were performed. The test specimens were  $55 \times 18.1 \times 6.3 \text{ mm}^3$ . An Instron tensile test machine was used. The elongation of the specimen was measured by an internal displacement gage. Thus, the accuracy is expected to be low. Specimens were moved from an oven or a freezer to the test machine and the tests were performed in a room temperature environment. Approximately 30 s were needed until the tensile test begun. The test was completed within an additional 2 - 3 s at the highest elongation rate and around 300 s at the lowest elongation rates. In the latter case the temperature of the specimen was significantly affected during the experiment. There were also considerable amounts of heat generated during the deformation.

Figure 6.1 shows an example of tensile test curves. All three tests in this case were performed at room temperature. Young's modulus,  $E$ , was calculated as stress versus strain at 25% of the fracture strength. Fracture strength is here defined as the maximum (engineering) stress obtained during the test. Fracture strain is defined as the strain when the maximum stress is obtained. The influence of elongation rate on  $E$  was not measurable. It is further noted that, for all elongation rates and all temperatures used in the study, the fracture strength decreases with increasing strain rate.

Figure 6.2 shows a noteworthy decrease in stiffness with temperature.  $E$  decreases more than a factor of 3 - 5 in the temperature range  $-30^\circ\text{C}$  to  $100^\circ\text{C}$ . A encouraging observation is that  $E$  seems to be fairly insensitive to temperature changes in the temperature range  $-30^\circ\text{C}$  to  $20^\circ\text{C}$  for both PP1 and PP2 when the fibre content is 40%.

A detrimental decrease of fracture strain with increasing fibre contents is observed in Fig. 6.3. A strong effect of strain rate is observed especially at 40% fibre content. Here the fracture strain decreases to almost 50% when the strain rate,  $d\epsilon/dt$ , increases from 0.001 to 0.01. The decreased fracture strain would have some impact on the fracture toughness of the material because of its connected the energy needed to create new surfaces in the material. Thus, it correlates with the product of fracture strength and fracture strain. This leads us to believe that the fracture toughness of the material is significantly reduced at higher fibre content. A detrimental decrease of fracture strain with increasing fibre contents is observed in Fig. 6.3. A strong effect of strain rate is observed especially at 40% fibre content. Here the fracture strain decreases to almost 50% when the strain rate,  $d\epsilon/dt$ , increases from 0.001 to 0.01. The decreased fracture strain would have some impact on the fracture toughness of the material the strain rate,  $d\epsilon/dt$ , increases from 0.001 to 0.01. The decreased fracture strain would have some impact on the fracture toughness of the material

because of its connected the energy needed to create new surfaces in the material. Thus, it correlates with the product of fracture strength and fracture strain. This leads us to believe that the fracture toughness of the material is significantly reduced at higher fibre content.

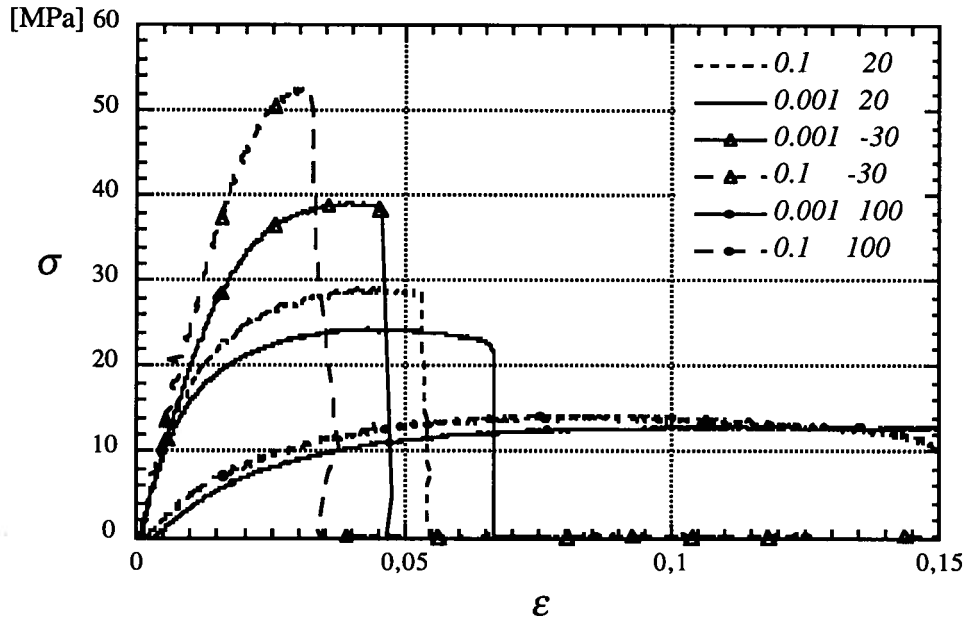


Fig. 6.1. Tensile tests performed on PP1 with a 20% fibre content. Two different strain rates were used at three different temperatures.

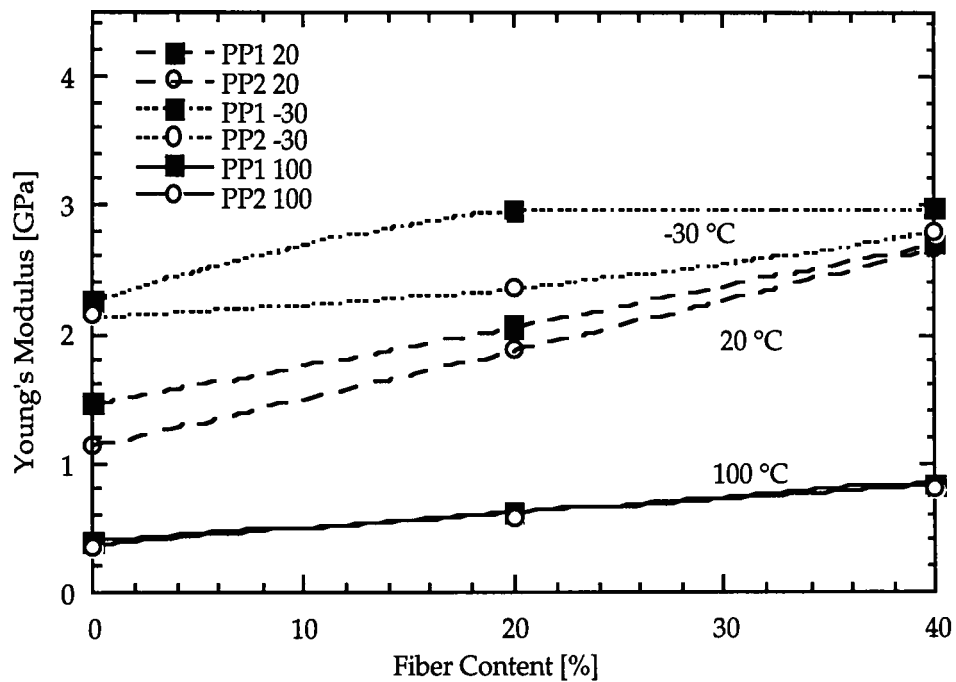


Fig. 6.2. Young's modulus obtained at different temperatures. The strain rate  $d\epsilon/dt=0.1$ .

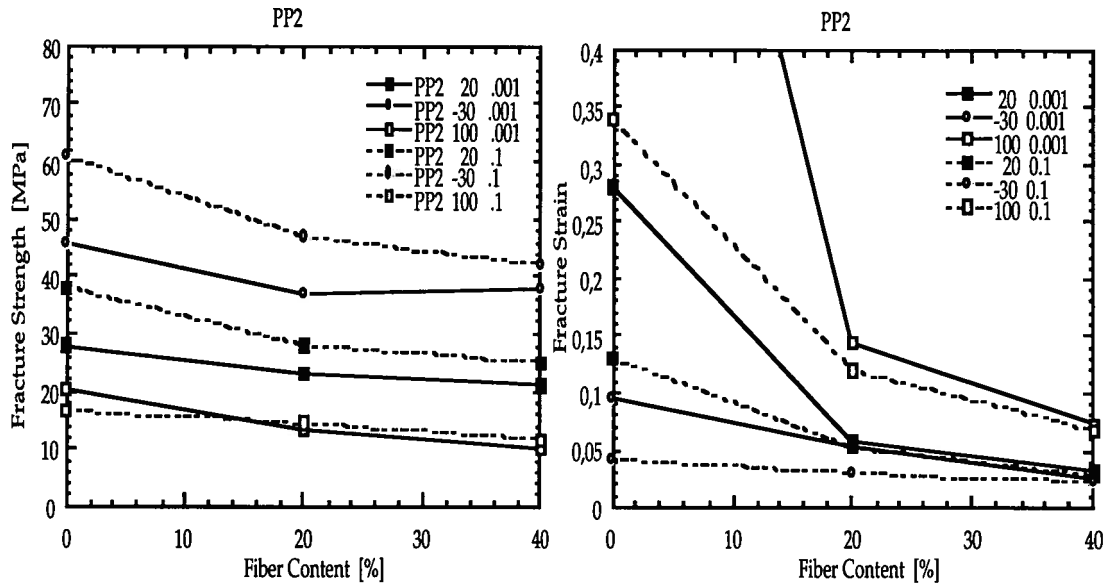


Fig. 6.3. a) Tensile strength obtained at different strain rates. b) Fracture strain obtained at different strain rates. The tests were performed at the temperatures -20, 20 and 100 °C.

## 7. Tensile Strength at Increased Humidity

The object of the tests performed at the, was to study the moisture sensitivity of materials. Test specimens measuring  $118 \times 22 \times 6 \text{ mm}^3$  were conditioned in three different climates: 50% RH 20°C (constant room), 97% RH 20°C ( $\text{K}_2\text{SO}_4$ ) and 100% RH 20°C (under water) for 45 days. In addition, special tensile specimens were stored at 50% and 100% RH for the same period. All test specimens were weighed and measured before and after conditioning. Change in length was measured with a micrometer gauge of 0.005 mm accuracy. A mean of three measurements was calculated since it was found difficult to measure the length exactly. The standard deviation varies between 0 and 0.02 mm which is in most cases less than the changes in length. Curvature was measured with a micrometer gauge mounted on a plate. The test specimens were weighed with an accuracy of 0.001 g before climatic exposure, after 30 days and after 45 days. The tensile specimens, shaped to have a waist, were subjected to tension in a 20 kN tensile test machine. The time for a tensile test was ca 30 s which may be regarded as rapid loading.

In all cases except one, conditioning of test specimens at 97% and 100% RH resulted in a change in moisture content. In Fig. 7.1, the change is shown in terms of kg of water per  $\text{m}^3$  of material (volume calculated at 50% RH). Weighing of the test specimens on three occasions shows that all specimens except PP1 and PP2 with 40% wood fibre were fully conditioned.

Length measurements before and after conditioning show that both PP1 and PP2 with 0% and 20% wood fibre shorten as a result of moisture loading

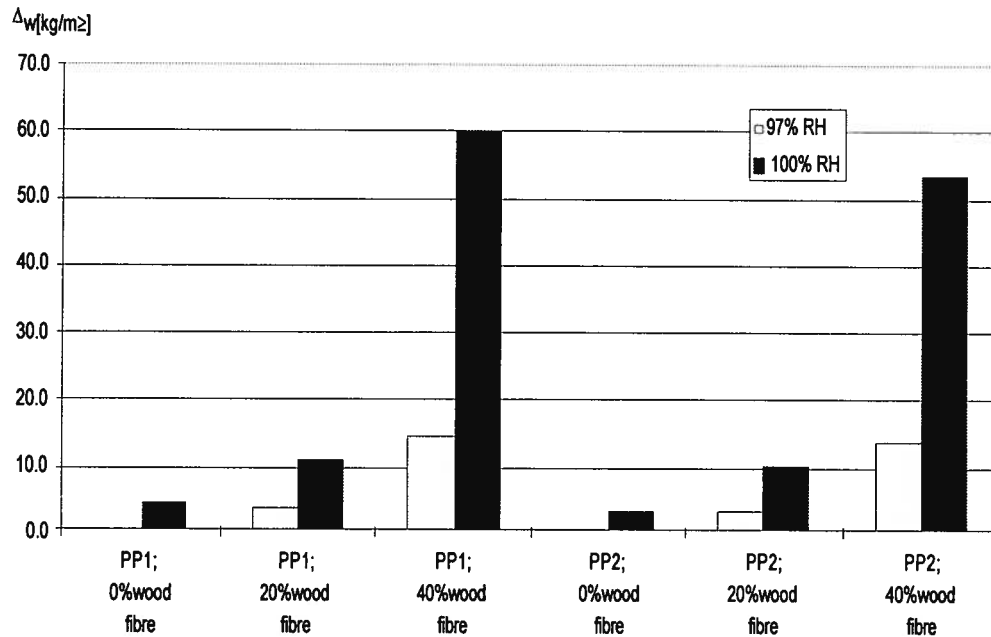


Fig. 7.1. Change in moisture content for six materials conditioned in two different climates for 45 days

The changes in length are however quite near the standard deviation for the measurements, which implies uncertainty. The results are nevertheless interesting since a consistent shrinkage occurred. PP1 and PP2 with 40% wood fibre, on the other hand, exhibited a distinct increase in length. At 100% RH the length of these specimens increased by over 0.2% which is equivalent to ca 5 mm over a 2 m long board. The changes in length for all materials conditioned at 97% and 100% RH are shown in Fig. 7.2. Longer test specimens would have been desirable to enable measurement errors and actual changes in length to be more easily distinguished.

Experiments were also made to study the propensity of the different materials to bend. In order that moisture load should be applied on only one side, two of three test specimens of each material and climate were coated with a thin layer of epoxy. In addition, one of these specimens was ground down to a thickness of 2 mm. The thin pieces (2 mm) exhibited visible curvature deformations, with the pure plastics materials (PP1 and PP2 with 0% wood fibre) bending with the epoxy side on the inside and the plastics side on the outside, while the test specimens with 40% wood fibre exhibited the opposite behaviour, i.e. they bent with the wood side on the inside. This is in direct contrast to the results from the measurements of the change in length! No reasonable explanation has as yet been found. Note that the results of changes in length and weight (Fig. 7.1 and 7.2) are based on 'clean' test specimens, i.e. those without epoxy.

The results of tensile tests are given in Fig. 7.3 as a value of the tensile strength of each material conditioned at 50% and 100% RH.

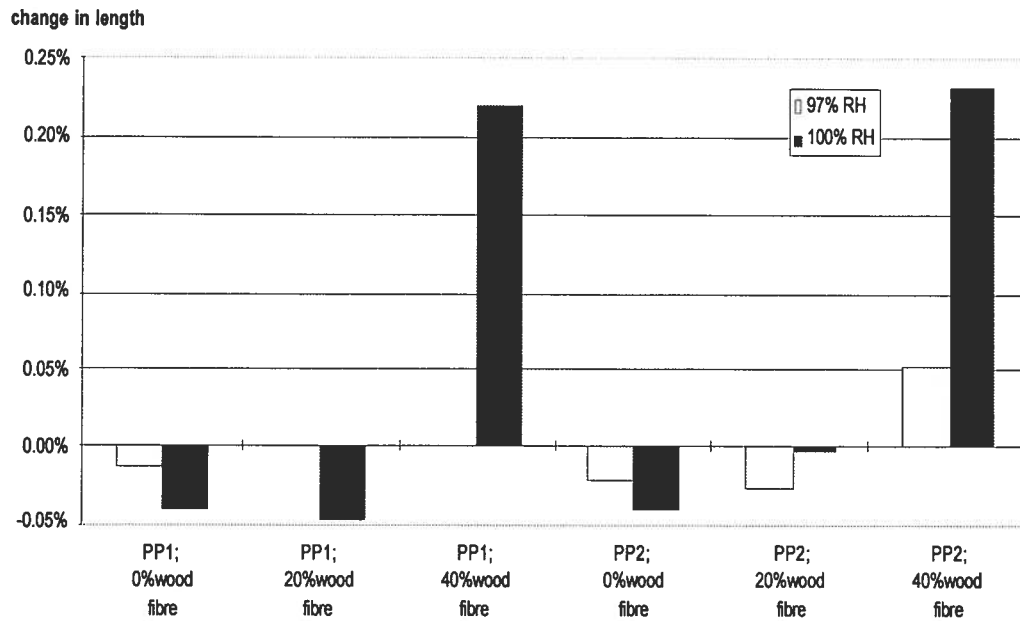


Fig. 7.2. Change in length as a percentage of the original length

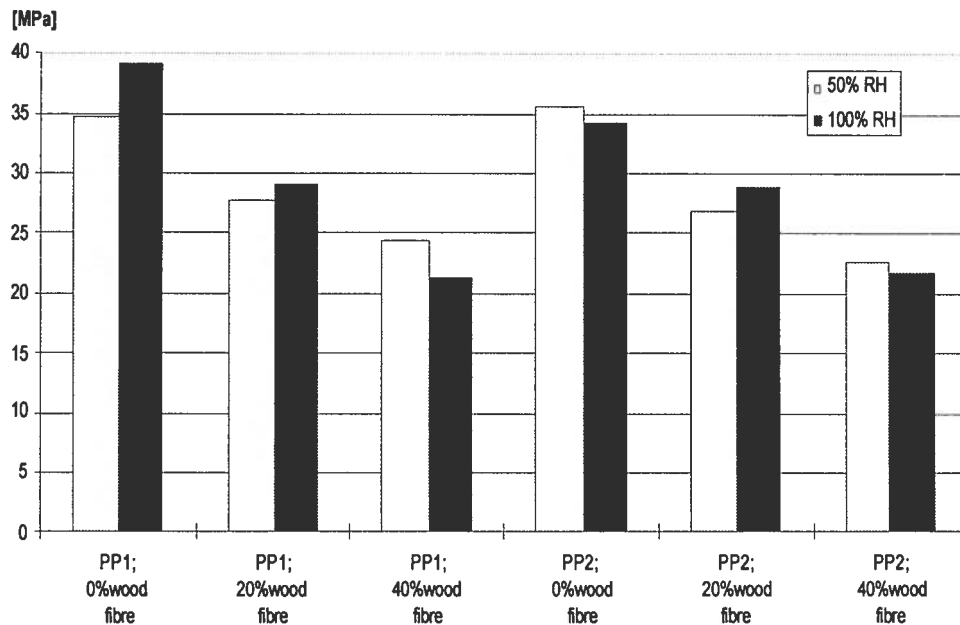


Fig. 7.3. Tensile strength of the different materials, obtained in tensile tests

The stiffness of the materials was determined using the dynamic Young's modulus. These experiments yielded unreasonably high values and are therefore not reported. This may be interpreted to mean that determination of Young's modulus with this method is not applicable to these materials.

Moisture loading produced no visible changes in the test specimens.



## 8. Conclusions

Several interesting conclusions emerge from the round robin tests. First the measurements of Young's modulus of the different material combinations at room temperature seem consistent. Young's modulus measured by Solid Mechanics, LTU (cf. section 6) are constantly lower than the other two groups (Structural Mechanics, LTH, section 5, and Experimental Mechanics, LTU, section 3), which may be because of a different definition of Young's modulus (at 25% of the fracture strength). Young's modulus measured by Structural Mechanics, LTH for PP1-40% seem somewhat high compared with the results from the other groups. We can also conclude that the effect on Young's modulus of increasing the fibre content from 0% to 20% and from 20% to 40% is an increase of 60% and 40% in stiffness, respectively. Poisson's ratio was only measured by one group and as expected it dropped from approximately 0.4 for the pure plastic materials to 0.3 at a fibre content of 40%. We conclude that the mechanical properties of the wood composites are determined by the wood content. The choice of matrix material seem to have no significant effect on neither Young's modulus nor Poisson's ratio.

The measurement of the anisotropy performed by Experimental Mechanics, LTU is not consistent with the measurement of the fibre angle by Wood Technology, LTU (cf. section 2.3). In the modal analysis a significant anisotropic effect was observed in the wood samples while on the other hand the fibres were determined to be randomly distributed at the surfaces of the sample. Since the surfaces carries most of the load in bending, and hence have the most impact on the modal shape, no significant anisotropy was expected. A more profound investigation of this discrepancy is therefore needed.

The behaviour of the material when exposed to moisture may not be acceptable or does at least limit the versatility of the material as members of structural components (Building Materials, CTH, section 7). The contradictory behaviour of the material when exposed to a homogeneously distributed moisture and when there would supposedly be a gradient of moisture content sow some doubt in the test method whereas no reasonable explanation has been found.